

Cooperative decentralized reactive circumnavigation of unpredictably moving and deforming speedy extended objects[★]

A. Matveev^{*,**} V. Magerkin^{*}

^{*} Department of Mathematics and Mechanics, Saint Petersburg University,
Saint Petersburg, Russia (e-mail: almat1712@yahoo.com).

^{**} Department of Control Systems and Industrial Robotics, Saint-Petersburg
National Research University of Information Technologies Mechanics and
Optics (ITMO), Saint Petersburg, Russia.

Abstract: A team of speed- and acceleration-limited robots travel in a plane that hosts an unpredictably moving and deforming extended targeted object. In its local frame, every robot has access to its own velocity and is able to identify the relative coordinates of the objects within a given finite visibility range, as well as the nearest point of the object. A sliding mode communication-free sensor-based strategy is presented that drives the robots to a desired distance from the targeted object and ensures its subsequent circumnavigation with maintaining this distance and effective self-distribution around the object. The proposed control law individually operates at any robot and is reactive, i.e., it directly converts the current sensory data into the current control in a reflex-like fashion. The performance of the proposed navigation law is rigorously justified by a global convergence result and is confirmed via computer simulation tests.

Keywords: Mobile robots, Circumnavigation, Nonlinear control, Sensor-based navigation

1. INTRODUCTION

Over the past decades formation control has become a mature research field, and its focus has been much shifted to the decentralized control paradigm and the issue of communication and sensorial limitations. In this area, much effort has been devoted to the problem of driving multiple mobile robots into a formation encircling a targeted object, see, e.g., (Kim and Sugie, 2007; Kawakami and Namerikawa, 2009; Kim et al., 2010; Kobayashi and Hosoe, 2011; Yamaguchi, 2003; Kothari et al., 2013; Tsumura et al., 2011; Ceccarelli et al., 2008; Guo et al., 2010). Motivation of this problem comes from many sources, such as rescue operations, exploration and surveillance, minimization of security risks, deployment of mobile sensor networks (Savkin et al., 2015), escorting missions, etc. Within this diversity, the targeted object has various incarnations, e.g., this may be a single body or a group of them, the concerned body can be treated as a point in some cases, whereas in others it should be handled as a moving and deforming 2D entity.

In such missions, the robots should approach the object and arrive at positions that are advantageous for mission running. The locus of them is often the *equidistant curve*, i.e., the set of points at a given distance from the object. After arrival at this curve, the robots should repeatedly trace it, thus circumnavigating the object. Typically, they should also surround the object from all sides and distribute themselves somewhat uniformly.

Up to now, research on robotic circumnavigation was mostly focused on point-wise targets. A single moving target is treated in (Kobayashi and Hosoe, 2011) for fully actuated robots, assuming access to the velocity vector of the target. For Hilare-type

robots, (Yamaguchi, 2003) provides an evidence of the team's local stability in closed-loop, but no rigorous convergence result is given. Assuming that the target obeys a known escaping rule, (Tsumura et al., 2011) gives conditions under which a linear control law drives identical linear agents with full actuation and observation into a target-centric formation. The cyclic pursuit pattern is used in (Kim and Sugie, 2007) to ensure capturing a moving target in 3D at a given altitude provided that there is an access to the target's velocity vector. For a steady target, basic findings of (Kim and Sugie, 2007) are extended to stable identical under-actuated vehicles in (Kim et al., 2010).

Cyclic-pursuit involves a steady ring-like information-flow graph. More general graphs are treated in (Kawakami and Namerikawa, 2009) for a moving target with measurable velocity. In (Kothari et al., 2013; Sato and Maeda, 2010), similar research is reported, with assuming uncertainties in data on the target or transmitted information, whereas the information-flow is independent of robots' motion. A more realistic case is examined in (Guo et al., 2010), where every robot observes its current predecessor and follower in the angular order around a moving target. Unlike the above papers, (Ceccarelli et al., 2008) deals with a finite range of visibility and justifies local stability of the uniform formation around a steady target. For an unpredictable speedy target and speed- and acceleration-limited robots with a finite visibility range, it is proved in (Matveev and Ovchinnikov, 2019) that the proposed decentralized control law drives the robots to a pre-specified distance to the target and ensures their even distribution around the target and a given common angular velocity of rotation about the target.

Circumnavigation of multiple targets has been studied only for point-wise ones and a single pursuer. In (Deghat et al., 2015), the simple-integrator robot is driven to and then along a circle

^{*} This work is supported by the Russian Science Foundation under the grant 19-19-00403.

centered at the mean of the targets' positions. For a Dubins-car-like robot, the controller from (Matveev et al., 2016) drives the root mean square distance (RMSD) to speedy targets to a given value. In (Matveev et al., 2017), a similar result is obtained in the case where RMSD is replaced by the distance to the nearest target. As for extended targets, circumnavigation of a steady 2D body by Dubins-car-like robots, along with their even self-distribution, is treated in (Ovchinnikov et al., 2015); circumnavigation of an arbitrarily moving and deforming object by a single such a robot is studied in (Matveev et al., 2012).

Meanwhile, the problem of circumnavigating a dynamic extended object by many robots lies in an uncharted territory. To fill this gap, we consider a speedy and unpredictably moving and deforming planar body. There is a team of point-wise robots, each driven by the acceleration vector. This vector and robot's velocity are upper bounded in magnitude. In its local frame, any robot has access to the positions of the peers within a finite visibility range, the nearest point of the body, and robot's own velocity, but cannot assess the speeds of any other elements in the scene or distinguish between the peers; the robots do not communicate. They should approach the body to a given distance, then trace the associated equidistant curve, and ultimately achieve an effective distribution over it.

We unveil conditions necessary for the mission to be feasible. A decentralized control law is then presented that under a slight enhancement of these conditions, solves the mission and excludes collisions of the robots with one another and the targeted body. This is shown via a rigorous global convergence result and is confirmed by computer simulation tests. That law combines event-based switching among discrete modes with nonlinear regulation within every mode, is reactive, but nevertheless is endowed with the capacity of global convergence.

The body of the paper is organized as follows. Sect. 2 describes the problem. Sect. 3 offers necessary conditions for the mission feasibility and assumptions. The control law and main results are given in Sects. 4 and 5, respectively. Sect. 6 reports on computer simulations, Sect. 7 offers conclusions. Due to the paper length limitation, the proofs of the presented results will be given in its full version.

2. PROBLEM FORMULATION

We consider a team of N robots moving in a plane and labeled 1 through N . Robot i is actuated by the acceleration, whose magnitude and the robot's speed do not exceed given bounds $\bar{a}_i > 0$ and $\bar{v}_i > 0$, respectively. In its local frame, the robot has access to its own velocity and is able to identify the relative coordinates of the objects within a given finite visibility range. Meanwhile, the robots are anonymous to one another (i.e., cannot distinguish between the peers) and cannot communicate.

There is an unpredictably moving 2D continuum $D = D(t) \subset \mathbb{R}^2$. Its moving pattern may be arbitrary; e.g., $D(t)$ may not only translate and rotate but also deform, i.e., change its shape via, e.g., stretching, skewing, motions of some parts relative to the others, etc. Starting from occasional locations, all robots should approach $D(t)$ to a common and given distance d_0 , then maintain it, encircle $D(t)$ in a common pre-specified direction (clockwise/counterclockwise), and achieve an effective self-distribution around $D(t)$, e.g., an even one, thus building a dynamic barrier around $D(t)$. In its local frame, every robot can find the nearest point of $D(t)$ and so the distance to $D(t)$.

We use the double integrator model of robot i :

$$\ddot{\mathbf{r}}_i = \mathbf{a}_i, \quad a_i := \|\mathbf{a}_i\| \leq \bar{a}_i, \quad \|\mathbf{v}_i(0)\| \leq \bar{v}_i. \quad (1)$$

Here \mathbf{r}_i is the position of the robot, \mathbf{v}_i is its velocity, the acceleration \mathbf{a}_i is the control input, and $\|\mathbf{w}\| := \sqrt{\langle \mathbf{w}; \mathbf{w} \rangle}$ and $\langle \cdot; \cdot \rangle$ are the Euclidean norm and inner product, respectively. The equation in (1) holds if the speed $v_i := \|\mathbf{v}_i\| \leq \bar{v}_i$. The controller must respect this condition; so discussion of effects above this bound or when trespassing it is of no relevance.

We do not specify whether the body is rigid, elastic, or plastic, or liquid, etc.; moreover, it may be a non-physical body, like an estimated area of potential threats. So we adopt only a few minimal conventions, typical for the continuum mechanics (Spencer, 2004). To state them, we follow the Lagrangian approach and so introduce a *reference configuration* $D_* \subset \mathbb{R}^2$ and a time-dependent *configuration map* $\Phi(\cdot, t)$ that converts D_* into the *current configuration* $D(t) = \Phi[D_*, t]$.

Assumption 1. The reference configuration D_* is compact and bounded by a C^2 -smooth and C^3 -piece-wise smooth Jordan curve; $\Phi(\cdot, t)$ is C^3 -smooth, one-to-one, and defined on an open vicinity O_* of D_* , its Jacobian matrix is everywhere invertible.

The velocity and acceleration of a moving particle $\mathbf{q} = \mathbf{q}(t) \in D(t)$ are defined as $V(\mathbf{q}, t) := \frac{\partial \Phi}{\partial t}[\mathbf{q}_*, t]$ and $A(\mathbf{q}, t) := \frac{\partial^2 \Phi}{\partial t^2}[\mathbf{q}_*, t]$, where $\mathbf{q}_* \in D_*$ is the "seed" of this particle $\mathbf{q}(t) = \Phi(\mathbf{q}_*, t)$ (Spencer, 2004). We also use the following notations:

- $\mathbf{dist}_A[\mathbf{r}] := \inf_{\mathbf{r}' \in A} \|\mathbf{r}' - \mathbf{r}\|$, distance from \mathbf{r} to the set A ;
- $\mathbf{p}_i(t) := \pi[\mathbf{r}_i(t), t]$, where $\pi(\mathbf{r}, t)$ is the *projection* of \mathbf{r} onto $D(t)$, i.e., the point of $D(t)$ nearest to \mathbf{r} ;
- $d_i(t) := \mathbf{dist}_{D(t)}[\mathbf{r}_i(t)]$, distance from robot i to $D(t)$;
- ∂A , boundary of the set $A \subset \mathbb{R}^2$;
- \mathbf{w}^\perp , vector \mathbf{w} rotated through $\pi/2$ counterclockwise;
- $[\boldsymbol{\tau}(\boldsymbol{\rho}, t), \mathbf{n}(\boldsymbol{\rho}, t)]$, right-handed Frenet frame of $\partial D(t)$ at $\boldsymbol{\rho} \in \partial D(t)$, the unit normal \mathbf{n} is directed inside $D(t)$;
- $W_\tau(\boldsymbol{\rho}, t) := \langle W; \boldsymbol{\tau}(\boldsymbol{\rho}, t) \rangle$, $W_n(\boldsymbol{\rho}, t) := \langle W; \mathbf{n}(\boldsymbol{\rho}, t) \rangle$, tangential and normal projections of vector W ;
- $\varkappa(\boldsymbol{\rho}, t)$, signed curvature of $\partial D(t)$ at point $\boldsymbol{\rho} \in \partial D(t)$;
- $V_r'(\mathbf{r}, t)$, spatial velocity gradient tensor;
- $\Omega(\mathbf{r}, t)$, *spin* (angular velocity of the rigid-body rotation) of the continuum $D(t)$, i.e., $\frac{1}{2}[V_r' - (V_r')^\top] = \begin{pmatrix} 0 & -\Omega \\ \Omega & 0 \end{pmatrix}$;
- $E(\mathbf{r}, t) := \frac{1}{2}[V_r' + (V_r')^\top]$, *strain-rate tensor* of $D(t)$;
- $\lambda(\mathbf{r}, t) := \langle E\boldsymbol{\tau}; \mathbf{n} \rangle + \Omega = \langle V_r'\boldsymbol{\tau}; \mathbf{n} \rangle$, rotational velocity of an infinitesimally small arc of $\partial D(t)$ that is due to both the rigid-body rotation of the continuum (the addend Ω) and its shear deformation (the addend $\langle E\boldsymbol{\tau}; \mathbf{n} \rangle$);
- $\eta(\mathbf{r}, t) := \langle E\boldsymbol{\tau}; \boldsymbol{\tau} \rangle$, rate of stretch of such an arc;
- $\sigma = \pm 1$ gives the desired direction of circumnavigating the targeted body (counterclockwise/clockwise).

3. NECESSARY CONDITIONS AND ASSUMPTIONS

The control objective includes regulation of the output d_i to the targeted value d_0 . *Local controllability* of the output is a classic prerequisite for feasibility of this goal: the output d_i can be both decreased and increased via proper controls. Since they directly affect only \dot{d}_i , this means that the sign of \dot{d}_i can be arbitrarily manipulated whenever $\dot{d}_i = 0$. We assume this only for motion at the maximal speed and in the *operational zone*, which is defined in terms of the distance d to $D(t)$:

$$Z_{\text{op}} := \{(\mathbf{r}, t) : d_- < d < d_+\}, \quad \text{where } d_- < d_0 < d_+ \quad (2)$$

are given. As is discussed in (Matveev et al., 2012), this assumption includes (up to tiny details) the following part.

Assumption 2. At any time t and for any point $\boldsymbol{q} \in \partial D(t)$,

$$0 < 1 + \varkappa(\boldsymbol{q}, t)d_{\text{-sgn } \varkappa}. \quad (3)$$

Also, the zone Z_{op} does not contain points \boldsymbol{r} for which the distance to $D(t)$ is furnished by multiple points of $D(t)$.

Further, we omit the argument (\boldsymbol{q}, t) in $\varkappa, V_\tau, V_n, A_n$.

Lemma 1. Let Asm. 2 hold. The output d_i is locally controllable in Z_{op} when moving at the maximal speed if and only if at any time t and for any $\boldsymbol{q} \in \partial D(t)$ and $d \in [d_-, d_+]$,

$$|V_n| < \bar{v}_i, \quad (4)$$

$$\left| A_n + \frac{2\lambda\xi + \varkappa\xi^2 - d\lambda^2}{1 + \varkappa d} \right| < \bar{a}_i \sqrt{1 - V_n^2/\bar{v}_i^2}, \quad (5)$$

$$\text{where } \xi := -V_\tau \pm \sqrt{\bar{v}_i^2 - V_n^2}. \quad (6)$$

The posed control objective consists of two parts: regulating the distance to $D(t)$ and that between the robots, respectively. These parts are concerned with the normal $v_{i,n}$ and tangential $v_{i,\tau}$ velocities, respectively. (The latter is true if all robots have attained the first goal and so are traveling near the d_0 -equidistant curve $\mathcal{E}(t) := \{\boldsymbol{r} : \text{dist}_{D(t)}[\boldsymbol{r}] = d_0\}$.) In order that the two regulated distances be independently controllable, we highlight the bounds $v_{i,\tau} \in [-\sqrt{\bar{v}_i^2 - v_{i,n}^2}, \sqrt{\bar{v}_i^2 - v_{i,n}^2}]$ that $v_{i,n}$ imposes on $v_{i,\tau}$. We demand that via these bounds, $v_{i,n}$ cannot induce an insurmountable trend in $v_{i,\tau}$: the gap between $v_{i,\tau}$ and both the upper and lower bound can be driven to any direction via a feasible acceleration without prejudice to d_i -controllability if $\|\boldsymbol{v}_i\| < \bar{v}_i$. We request this only on $\mathcal{E}(t)$.

Meanwhile, $v_{i,n}$ and $v_{i,\tau}$ are directly affected by the respective components $a_{i,n}$ and $a_{i,\tau}$ of the control \boldsymbol{a}_i . To not leave \mathcal{E} , these components should neutralize the matching parts of the centripetal and Coriolis accelerations and the own acceleration of the curve \mathcal{E} . With the formulas for these accelerations in mind, we see that allotment of the available control effort \bar{a} among normal $a_{i,n}$ and tangential $a_{i,\tau}$ directions depends on the speeds and accelerations of the points of \mathcal{E} . However, their evaluation is often a hard challenge in practical setting. This motivates control solutions that do not call for resolving this challenge and are based on a situation-independent allocation of the control effort. To sum up, we denote the above gap by

$$g_{\pm,i} := v_{i,\tau} \pm \sqrt{\bar{v}_i^2 - v_{i,n}^2}. \quad (7)$$

Definition 1. Robot i is said to be *locally controllable at a distance of d_0 from $D(t)$ with situation-independent allotment of the control effort* if there are $\bar{a}_{i,\tau}, \bar{a}_{i,n} > 0$ such that $\bar{a}_{i,\tau}^2 + \bar{a}_{i,n}^2 \leq \bar{a}_i^2$ and whenever the robot travels over \mathcal{E} (i.e., $\boldsymbol{r}_i(t) \in \mathcal{E}(t) \forall t$) with a speed of $v_i < \bar{v}_i$, the following holds:

- i) The signs of \ddot{d}_i and $\dot{g}_{\pm,i}$ (with any sign drawn from \pm) can be freely manipulated via normal $a_i^n \in [-\bar{a}_{i,n}, \bar{a}_{i,n}]$ and tangential $a_i^\tau \in [-\bar{a}_{i,\tau}, \bar{a}_{i,\tau}]$ accelerations, respectively, if the other acceleration is in the indicated interval.

Lemma 2. Suppose that robot i has the trait introduced by Defn. 1. Then there are $\bar{a}_{i,\tau}, \bar{a}_{i,n} > 0$ such that $\bar{a}_{i,\tau}^2 + \bar{a}_{i,n}^2 \leq \bar{a}_i^2$, (5) is true with $\bar{a}_i := \bar{a}_{i,n}, d := d_0, < \mapsto \leq$, and for any time t and point $\boldsymbol{q} \in \partial D(t)$, the following two conditions hold:

$$2 \frac{|\lambda - \varkappa V_\tau| + |\varkappa| \sqrt{\bar{v}_i^2 - V_n^2} |V_n|}{1 + d_0 \varkappa} + \frac{\bar{a}_{i,n} |V_n|}{\sqrt{\bar{v}_i^2 - V_n^2}} \leq \bar{a}_{i,\tau}, \quad (8)$$

$$|\lambda^2/\varkappa - A_n| < \bar{a}_{i,n} \text{ if } |\lambda - \varkappa V_\tau| < |\varkappa| \sqrt{\bar{v}_i^2 - V_n^2}. \quad (9)$$

Conversely, if all these conditions are true with $\leq \mapsto <$ everywhere, the above trait does appear.

Now we slightly enhance the above necessary conditions.

Assumption 3. There are $\Delta_d, \Delta_v, \Delta_a, \Delta_a^\tau, \Delta_a^n > 0$ such that for any robot, (3), (4), (5) remain true if their r.h.s. are decreased by $\Delta_d, \Delta_v, \Delta_a$, respectively. The conditions from Lem. 2 are true even if $\bar{a}_{i,n}$ is replaced by $\bar{a}_{i,n} - \Delta_a^n$ and $\bar{a}_{i,\tau}$ by $\bar{a}_{i,\tau} - \Delta_a^\tau$.

Here the constants Δ (with various indices) are taken common for all robots only for ease of notation. This does not limit generality since passing to the minimum (over all robots) of the eponymous individual constants keep Asm. 3 true.

Asm. 3 is true if $\bar{v}_i, \bar{a}_{i,n}, \bar{a}_{i,\tau}, \Delta_v, \Delta_a, \Delta_a^\tau, \Delta_a^n$ are slightly and coherently reduced. We do this to ensure that \bar{v}_i is a feasible speed and $\bar{a}_{i,n}^2 + \bar{a}_{i,\tau}^2 \leq \bar{a}_i^2 - \Delta_{aa}$ with some $\Delta_{aa} > 0$.

Assumption 4. The map $\Phi(\cdot)$ from Asm. 1, its derivatives up to the third degree, and the inverse to the spatial Jacobian matrix $\Phi'_q(\cdot)$ are bounded on the domain of definition $O_* \times [0, \infty)$.

In its local frame, robot i can determine its own projection $\boldsymbol{q}_i(t)$ onto the body $D(t)$ and so can find $\boldsymbol{q}_i(t) - \boldsymbol{r}_i(t) = d_i(t)\boldsymbol{n}[\boldsymbol{q}_i(t), t]$, $d_i(t) = \|\boldsymbol{q}_i(t) - \boldsymbol{r}_i(t)\|$, and

$$\boldsymbol{q}_i^{d_0}(t) := \boldsymbol{q}_i + d_0/d_i(t)[\boldsymbol{r}_i(t) - \boldsymbol{q}_i(t)] \in \mathcal{E}(t). \quad (10)$$

Assumption 5. The visibility ranges of the robots are such that there exist $\Delta_{\text{vis}}^d, \Delta_{\text{vis}}^s > 0$ for which the following claim holds:

- Whenever $|d_i(t) - d_0|, |d_j(t) - d_0| \leq \Delta_{\text{vis}}^d$ and the arc of $\mathcal{E}(t)$ between $\boldsymbol{q}_i^{d_0}(t)$ and $\boldsymbol{q}_j^{d_0}(t)$ does not exceed Δ_{vis}^s in length, robot i “sees” robot j and the entirety of this arc.

The main part of the maneuver, where the proposed control law is put in use, is prefaced by a surely performable preliminary part. We drop discussion of rather trivial details of its implementation and merely state the needed outcome of this part.

Assumption 6. The following claims hold initially. Every robot i 1) has been pushed up to the maximal speed \bar{v}_i , 2) has been steered far enough from the targeted domain: $D(0)$ and $\boldsymbol{r}_i(0)$ are separated by a straight line L_i and $\text{dist}_{L_i}[\boldsymbol{r}_i(0)] > (3\pi + 2)\bar{v}_i^2/\bar{a}_i + d_0$, and 3) the disc with a radius of $2\bar{v}_i^2/\bar{a}_i$ centered at $\boldsymbol{r}_i(0)$ remains in Z_{op} from $t = 0$ to $t = 3\pi\bar{v}_i/\bar{a}_i$. Also, 4) the robots have been moved to locations that are far enough from one another: $\|\boldsymbol{r}_i(0) - \boldsymbol{r}_j(0)\| > 6\pi \max_k \bar{v}_k^2/\bar{a}_k \forall i \neq j$.

The relation (4) implies that it suffices to move with a constant velocity and top speed to ultimately get in 2). Distinct orientations of the velocities for various robots yield 4). The claim 3) is in fact about the choice of d_\pm in (2).

4. PROPOSED NAVIGATION LAW

The controllers of various robots implement a common rule and are hybrid. They pass through two discrete states:

$$\text{Go-to} \xrightarrow{|d_i - d_0| \leq d_\downarrow} \text{Cir}. \quad (11)$$

The state **Go-to** is initial and $d_\downarrow > 0$ is a parameter of the controller. In **Go-to**, the robot should arrive at the distance d_0 to $D(t)$ with the desired direction σ of motion around $D(t)$. In **Cir**, the robot should circumnavigate $D(t)$ over $\mathcal{E}(t)$ in this direction and take measures aimed at achieving and maintaining an effective distribution of the robots over $\mathcal{E}(t)$.

Discrete state “Go-to”. The control input \boldsymbol{a}_i is given by

$$\boldsymbol{a}_i = \sigma \bar{a}_i \cdot \text{sgn} \{ \dot{d}_i + \mu \chi[d_i] \} \boldsymbol{u}_i^\perp, \quad \text{where } \boldsymbol{u}_i := \boldsymbol{v}_i/v_i. \quad (12)$$

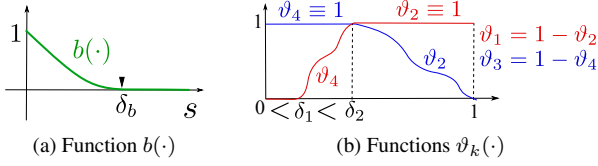


Fig. 1. Auxiliary functions used by the controller

Here $\mu > 0$ and a map $\chi(\cdot) \in \mathbb{R} \rightarrow \mathbb{R}$ is to be chosen by the designer of the controller, is smooth and such that

$$\begin{aligned} \chi(z) < 0 \quad \forall z < 0, \quad \chi(z) > 0 \quad \forall z > 0, \\ \bar{\chi} := \sup_{z \in \mathbb{R}} |\chi(z)| < \infty, \quad \bar{\chi}' := \sup_{z \in \mathbb{R}} |\chi'(z \pm)| < \infty. \end{aligned} \quad (13)$$

To assess the time derivative \dot{d}_i of the reading $d_i(t)$ any method is welcome; there is numerical differentiation among them.

Discrete state ‘‘Cir’’. Whenever $|d_i(t) - d_0| \leq \Delta_{\text{viz}}^d$, Asm. 5 guarantees that robot i can compute the signed (and counted in the direction of σ) length $s_{i \rightarrow j}(t)$ of the arc of $\mathcal{E}(t)$ between $\boldsymbol{q}_i^{d_0}(t)$ and $\boldsymbol{q}_j^{d_0}(t)$ for any close enough $|s_{i \rightarrow j}(t)| \leq \Delta_{\text{viz}}^s$ robot j with $|d_j(t) - d_0| \leq \Delta_{\text{viz}}^d$. We pick a special parameter $\Delta^s > 0$ and subject it, along with d_\downarrow from (12), to the bounds:

$$0 < d_\downarrow \leq \Delta_{\text{viz}}^d, \quad 0 < \Delta^s \leq \Delta_{\text{viz}}^s. \quad (14)$$

Definition 2. A close neighbor of robot i is robot $j \neq i$ such that $|d_j - d_0| < d_\downarrow$ and $|s_{i \rightarrow j}| < \Delta^s$. Such a neighbor is said to be forward/backward if $s_{i \rightarrow j} > 0/s_{i \rightarrow j} \leq 0$, respectively.

By the foregoing, robot i can identify its close neighbors and find $s_i := \min_j s_{i \rightarrow j} > 0$. Here \min_j is over all close forward neighbors j of i if they exist; otherwise, $s_i := \Delta^s$.

Apart from $\Delta^s > 0$, the designer should pick $\bar{a}_n, \bar{a}_\tau, \varkappa_b > 0$ and a smooth map $\Xi(\cdot) : [0, \Delta^s] \rightarrow \mathbb{R}$ for which

$$\Xi(0) \geq 0, \quad \Xi' := \min_{s \in [0, \Delta^s]} \Xi'(s) > 0. \quad (15)$$

The control input \mathbf{a}_i is given by

$$\begin{aligned} \mathbf{a}_i &= a_i^n \mathbf{e}_i - a_i^\tau \mathbf{e}_i^\perp, \quad \text{where } \mathbf{e}_i = (\boldsymbol{q}_i - \mathbf{r}_i) / \|\boldsymbol{q}_i - \mathbf{r}_i\|, \\ a_i^n &:= \bar{a}_{i,n} \cdot \mathbf{sgn}[\dot{d}_i + \mu \chi(d_i)], \\ a_i^\tau &:= -\bar{a}_{i,\tau} \cdot \mathbf{sgn}[\Sigma_i(s_i, t) - b_i^\Sigma], \\ \Sigma_i(s, t) &:= \vartheta_1 \dot{s}_i + \vartheta_2 v_{i,\tau} - \sigma \left[\vartheta_3 \sqrt{[\bar{v}_i^2 - v_{i,n}^2]_+} + \vartheta_4 \Xi(s) \right], \\ b_i^\Sigma &:= \zeta_b \sum_j b(s_j), \end{aligned} \quad (16)$$

$$\text{where } [b]_+ := \max\{b, 0\} \text{ and } \vartheta_k = \vartheta_k(|d_i|/d_\downarrow). \quad (18)$$

Here $\dot{s}_i := \left\langle \dot{\boldsymbol{q}}_i^{d_0}(t); \boldsymbol{\tau}[\boldsymbol{q}_i(t), t] \right\rangle$ is the tangential speed of $\boldsymbol{q}_i^{d_0}(t)$. The smooth maps $b(\cdot), \vartheta_k(\cdot)$ are to be chosen subject to the features displayed in Fig. 1, where $\delta_b > 0$ and $0 < \delta_1 < \delta_2 < 1$ are arbitrary. The forward close neighbors j of robot i are enumerated according to the remoteness of \boldsymbol{q}_j from \boldsymbol{q}_i ; the robots with a common \boldsymbol{q}_j (if exist) are numbered in ascending order of d_j . If $\mathbf{r}_k \neq \mathbf{r}_j \quad \forall k \neq j$, such an enumeration is unique. In (17), the sum \sum_j is from the least index to the first zero addend. (Any sum over the empty set is defined to be 0.)

Robot i can evaluate its own tangential $v_{i,\tau} = \langle \mathbf{v}_i; \boldsymbol{\tau}(\boldsymbol{q}_i, t) \rangle$ and normal $v_{i,n} = \langle \mathbf{v}_i; \mathbf{n}(\boldsymbol{q}_i, t) \rangle$ velocities since $\boldsymbol{\tau}(\boldsymbol{q}_i, t) = -\mathbf{e}_i(\boldsymbol{q}_i, t)^\perp, \mathbf{n} = \mathbf{e}_i(\boldsymbol{q}_i, t)$. Evaluation of $\dot{s}_i := \left\langle \dot{\boldsymbol{q}}_i^{d_0}; \boldsymbol{\tau}[\boldsymbol{q}_i, t] \right\rangle$ may be based on numerical differentiation of the computed

projection $\boldsymbol{q}_i^{d_0}$. However if \boldsymbol{q}_i and $\boldsymbol{\tau}$ are computed in the local frame F_i of robot i and the upper index l signals about attribution to F_i , then $\dot{s}_i = \left\langle \dot{\boldsymbol{q}}_i^{d_0,l}; \boldsymbol{\tau}^l[\boldsymbol{q}_i, t] \right\rangle + v_{i,\tau} - \varpi_i(d_i - d_0)$, where ϖ_i is the angular velocity of F_i . If the robot is close to \mathcal{E} , then $d_i \approx 0, \boldsymbol{q}_i^l \approx 0$ and, often similarly, $\dot{\boldsymbol{q}}_i^l \approx 0$. Then $\dot{s}_i \approx v_{i,\tau}$ and in (17), the sum of the first two addends $\approx v_{i,\tau}$.

The state $\mathbf{x} = \{(\mathbf{r}_i, \mathbf{v}_i)\}_{i=1}^N$ of the closed-loop system obeys an ODE $\dot{\mathbf{x}} = f(\mathbf{x}, t)$, where the r.h.s. is discontinuous; we consider Filippov’s solutions of this ODE. Since $\|f(\mathbf{x}, t)\| \leq k(1 + \|\mathbf{x}\|) \quad \forall \mathbf{x}, t$ with some $k > 0$, any solution is extendible to all $t \geq 0$ (Filippov, 1988). We do not discuss the more intricate issue of its uniqueness and address all solutions, except for unviable ones. The latter are those going on a repelling discontinuity manifold. Any state from this manifold gives rise to a solution going away from the manifold, also almost all arbitrarily small perturbations of this state cause inevitably ‘‘going away’’. So the solutions that go on the manifold do not occur in practice due to their utmost finite-horizon instability.

5. MAIN RESULTS

Theorem 1. Let Asm. 1–6 hold. Then the control law can be tuned so that the following is true for the closed-loop system:

- i) The robots respect the speed and acceleration bounds from (1), i.e., $\|\mathbf{v}_i(t)\| \leq \bar{v}_i$ and $\|\mathbf{a}_i(t)\| \leq \bar{a}_i$ for all i and t ;
- ii) The robots do not collide with one another and $D(t)$;
- iii) Every robot reaches the desired distance to the targeted body: $d_i(t) \rightarrow d_0$ as $t \rightarrow \infty$ for all i ;
- iv) Eventually, every robot travels along the d_0 -equidistant curve $\mathcal{E}(t)$ in the desired direction: $\sigma v_{i,\tau}(t) \geq \alpha$, where the constant $\alpha > 0$ does not depend on t and i ;
- v) Eventually, the robots maintain a certain order on $\mathcal{E}(t)$: after their proper enumeration from 0 to $N - 1$ and since some time, the projection $\boldsymbol{q}_i^{d_0}(t)$ of robot i onto $\mathcal{E}(t)$ is different from $\boldsymbol{q}_{i \oplus 1}^{d_0}(t)$ and immediately precedes this point on the loop $\mathcal{E}(t)$, where \oplus is addition modulo N ;
- vi) Suppose in addition that the body $D(t)$ is steady and the visibility zone of any robot contains a peer under even deployment of the robots over the equidistant curve: $\Delta_{\text{vis}}^s > P/N$. Here Δ_{vis}^s is taken from Asm. 5, P is the perimeter of \mathcal{E} and N is the number of the robots. Also, let $\Delta^s > P/N$ in (14). Then the robots’ distribution over \mathcal{E} is asymptotically even: $s_{i \rightarrow i \oplus 1} \rightarrow P/N$ as $t \rightarrow \infty$. Also, they sweep \mathcal{E} with a speed that goes to $\Xi(P/N)$ as $t \rightarrow \infty$.

Here v) means non-clustering. Harsh violation $\Delta_{\text{vis}} < P/N$ of the assumption $\Delta_{\text{vis}} > P/N$ from vi) implies that adjacent robots are invisible to each other under even deployment over \mathcal{E} . This makes the objective of even distribution hardly feasible since coming close to such distribution is inevitably accompanied by the loss of feedback from the inter-robot distances.

The reminder of the section is devoted to recommendations on controller tuning. In brief, it suffices to pick the parameters $d_\downarrow, \Delta^s, \mu, \delta_b, \zeta_b > 0$ small enough and the function $\Xi(\cdot)$ from (15) with sufficiently small slope and magnitude to ensure i)–v) in Thm. 1, whereas vi) additionally needs the lower bound $\Delta^s > P/N$. These can be viewed as guidelines for experimentally tuning the controller. Now we specify them by giving specific quantitative bounds. They refer to d_L from 2) in Asm. 6, d_\pm from (2), $\Delta_d, \Delta_v, \Delta_a^\tau, \Delta_a^n > 0$ from Asm. 3, as well as to the following bounds, which are finite due to Asm. 4:

$$|\zeta(\mathbf{q}, t)| \leq \bar{\zeta} \quad \forall \mathbf{q} \in \partial D(t), \forall t$$

$$0 < \underline{p} \leq \text{Perimeter of } \partial D(t) \leq \bar{p} \quad \forall t. \quad (19)$$

Here ζ assumes the following values $\varkappa, \lambda, \eta, V, A, \lambda'_\rho, \varkappa'_\rho, A'_\rho$, the symbol $'_\rho$ refers to the derivative in the tangential direction, and $|\zeta|$ should be replaced by $\|\zeta\|$ for $\zeta = V, A, A'_\rho$.

Thresholds d_\downarrow for (11) and Δ^s in Defn. 2 are such that (14) is true and for any robot i , the following inequalities hold, where $\alpha \in (0, 1)$ is arbitrarily chosen prior to d_\downarrow and Δ^s :

$$d_\downarrow < d_L - (3\pi + 2)\bar{v}_i^2/\bar{a}_i - d_0, \quad d_0 - d_-, \quad d_+ - d_0,$$

$$d_\downarrow < \frac{\Delta_d^3 \Delta_a^n}{2[\bar{\lambda} + \bar{\varkappa}(\bar{V} + \bar{v}_i)]^2}, (1 - \alpha) \frac{\Delta_d}{\bar{\varkappa}},$$

$$d_\downarrow < \left. \begin{aligned} & \frac{\alpha \Delta_d \sqrt{\bar{v}_i \Delta_v - \Delta_v^2/4}}{2\delta_2[\bar{\lambda} + \bar{\varkappa}(\bar{V} + \bar{v}_i)]}, \quad d_\downarrow \left\{ \bar{a}_i + 2 \frac{\bar{\lambda} + \bar{\varkappa}(\bar{V} + \bar{v}_i)}{\alpha \Delta_d} \bar{v}_i \right\} \\ & < \frac{\alpha \Delta_a^\tau \Delta_d}{6\bar{\varkappa}} \frac{\sqrt{\bar{v}_i \Delta_v - \Delta_v^2/4}}{\bar{v}_i + \sqrt{\bar{v}_i \Delta_v - \Delta_v^2/4}}, \end{aligned} \right\}$$

$$d_\downarrow(B_0 + B_1 d_\downarrow + B_2 d_\downarrow^2) < \frac{\alpha \Delta_a^\tau \Delta_d}{6\delta_2}, \text{ where}$$

$$B_0 := \bar{A}'_\rho + \bar{\varkappa} \bar{A} + \bar{\varkappa}^2 \bar{V}^2 + [\bar{\lambda}'_\rho + \bar{\varkappa}(\bar{\lambda} + \bar{\eta})] \bar{V} + B_\diamond \bar{v}_i \Delta_d$$

$$+ \frac{\bar{\lambda}(\bar{\eta} + d_0 \bar{\lambda}'_\rho) + \bar{\varkappa}'_\rho \bar{V}^2 + (\bar{\eta} \bar{\varkappa} + \bar{\lambda}'_\rho + \bar{\varkappa}'_\rho \bar{\lambda} d_0) \bar{V}}{\Delta_d},$$

$$B_1 := B_* \bar{v}_i \Delta_d + B_\diamond (\bar{\lambda} + \bar{\varkappa} \bar{V}), \quad B_2 := B_* (\bar{\lambda} + \bar{\varkappa} \bar{V}), \quad \text{and}$$

$$B_* := \frac{[\bar{\lambda} + \bar{\varkappa}(\bar{V} + \bar{v}_i)] \bar{\varkappa}'_\rho}{\alpha^2 \Delta_d^4},$$

$$B_\diamond := \frac{(2\bar{\lambda}'_\rho + 2\bar{\varkappa} \bar{\eta} + \bar{\varkappa}^2 \bar{V}) \Delta_d + \bar{\varkappa}'_\rho [\bar{V}(1 + \Delta_d) + \bar{v}_i + \bar{\lambda} d_0]}{\alpha \Delta_d^3}.$$

Due to 2) in Asm. 6, these are met by taking d_\downarrow small enough.

Function $\Xi(s)$ of $s \in [0, \Delta^s]$ is smooth and such that

$$\bar{\Xi} := \max_{s \in [0, \Delta^s]} \Xi(s) < \frac{1}{2} \sqrt{\bar{v}_i \Delta_v - \Delta_v^2/4},$$

$$\bar{\Xi}' := \max_{s \in [0, \Delta^s]} \Xi'(s) < \frac{\alpha \Delta_a^\tau \Delta_d}{6[2(\bar{v}_i \Delta_d + (\bar{\lambda} + \bar{\varkappa} \bar{V}) d_\downarrow) + \alpha \bar{p} \bar{\varkappa} \bar{v}_i]}.$$

These are met by, e.g., any nonnegative linear ascending function with sufficiently small slope and range.

Parameter μ is chosen by using $\bar{\chi}$ from (13) and upper bounds $\bar{\vartheta}'_k$ on $|\vartheta'_k(\zeta)|, \zeta \in [0, 1]$ for the maps from Fig. 1b. This parameter is chosen so small that

$$2\mu \bar{\chi} \leq \Delta_v, \quad \left[\frac{\bar{a}_i \sqrt{\bar{\chi}}}{\sqrt{\bar{v}_i}} + 2 \frac{(\bar{\lambda} + \bar{\varkappa} \bar{V}) \sqrt{\bar{v}_i \bar{\chi}}}{\Delta_d^2} \right] \sqrt{2\mu}$$

$$+ 2 \frac{\bar{\varkappa} \bar{v}_i \bar{\chi}}{\Delta_d^2} \mu + \bar{\chi} \bar{\chi}' \mu^2 < \Delta_a,$$

$$2\bar{v}_i \bar{\chi} \left[\left(1 + \frac{\bar{v}_i \mu \bar{\chi}}{\Delta_v^2} \right) \bar{\varkappa} + \frac{\bar{\lambda} + \bar{\varkappa} \bar{V}}{\Delta_v \Delta_d} \right] \mu + \bar{\chi} \bar{\chi}' \mu^2 < \frac{\Delta_a^n}{2},$$

$$\frac{\bar{\varkappa}(\bar{v}_i + \bar{\Xi}) \bar{\vartheta}'_3}{(1 - \alpha) \Delta_d} + \frac{\bar{v}_i^3 [\bar{a}_{i,n} \Delta_d + \bar{\lambda} + \bar{\varkappa}(\bar{V} + \bar{v}_i) \bar{v}_i]}{\Delta_d (\bar{v}_i \Delta_v - \Delta_v^2/4)^{3/2}}$$

$$+ \frac{(\bar{\vartheta}'_1 + 2) [\bar{\lambda} + \bar{\varkappa}(\bar{V} + \bar{v}_i)]}{\alpha^2 \Delta_d}$$

$$+ \left[\bar{\varkappa} + \frac{\bar{\lambda} + \bar{\varkappa}(\bar{V} + 2\bar{v}_i)}{\sqrt{\bar{v}_i \Delta_v - \Delta_v^2/4}} \right] \frac{\bar{v}^2}{\Delta_d \sqrt{\bar{v}_i \Delta_v - \Delta_v^2/4}} < \frac{\Delta_a^\tau}{6\mu \bar{\chi}}.$$

Parameter δ_b from Fig. 1a is chosen so small that

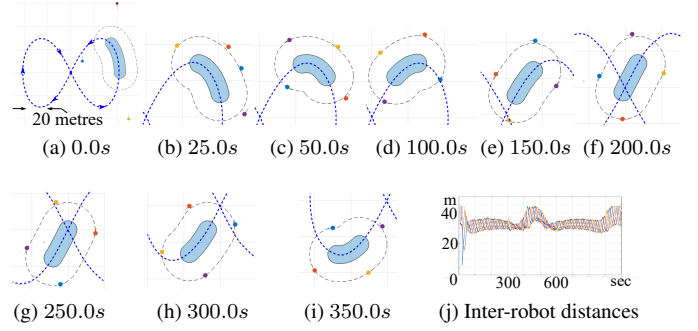


Fig. 2. A moving, bending, and resizing continuum.

$$\delta_b < \Delta^s/N, \underline{p}/N, \quad \text{where } \underline{p} \text{ is taken from (19).}$$

Parameter ζ_b from (17) is chosen by using Δ_{aa} (introduced in the second paragraph after Asm. 3) and is picked so small that

$$0 < \zeta_b < \Delta_a^\tau/(6N), \quad 2\bar{a}_i N \zeta_b + N^2 \zeta_b^2 < \Delta_{aa}.$$

Theorem 2. Let the assumptions of Thm. 1 hold and the parameters of the control law be chosen subject to the above recommendations. Then the claims **i)**—**v)** of Thm. 1 are true. If the additional assumptions of the claim **v)** from Thm. 1 hold and $\Delta^s := \Delta_{\text{vis}}$, the claim **vi)** is true as well.

6. RESULTS OF COMPUTER SIMULATION TESTS

The numerical values of the basic parameters used in the tests are listed in Table I, where τ is the control update period and the index i is dropped since the parameters are common for all robots i . The sensor readings were corrupted by noises evenly distributed over $[-0.01m, 0.01m]$. The two-point Newton quotient was used to estimate time-derivatives. Multimedia of extended versions of the tests are available at

https://drive.google.com/drive/folders/1jwoZW17Pd_-DCLVUUDyAFa20GahAqUEU?usp=sharing

Table I: Parameters used for simulation

$d_0 = 10.0m$	$\bar{a} = 3.0 \frac{m}{s^2}$	$\bar{v} = 5.0 \frac{m}{s}$	$\Delta_{\text{viz}}^s = 50.0m$
$\Delta_{\text{viz}}^d = 10.0m$	$\tau = 0.05s$	$\mu = 3.0 \frac{m}{s}$	$\chi(d) = \arctan \frac{d}{20}$
$\bar{a}^n = 2.0 \frac{m}{s^2}$	$\bar{a}^\tau = \sqrt{5} \frac{m}{s^2}$	$d_\downarrow = 3.5m$	$\Delta^s = 14\pi m$
$\Xi(z) = \frac{4z}{\Delta^s}$	$\delta_b = 0.2m$	$\delta_1 = \frac{1}{2} \delta_2 = \frac{1}{4}$	$\zeta_b = 0.002 \frac{m}{s^2}$

In Fig. 2–4, the robots are depicted as colored discs with short segments (to show the orientation of the velocity). The targeted body $D(t)$ is shown in blue; the path of its characteristic point is displayed as a dashed blue line in Fig. 2, 4. The targeted d_0 -equidistant curve $\mathcal{E}(t)$ is depicted as a black dashed curve.

In Fig. 2, the targeted body moves, bends and resizes. The path of its characteristic point is fully displayed in Fig. 2(a), only parts of this path are shown in Fig. 2(b–i). From the initial deployment in Fig. 2(a), the robots reach $\mathcal{E}(t)$ (in Fig. 2(b)) in $\approx 25.0s$, while not colliding with the body and one another. Then the robots trace the moving and deforming curve $\mathcal{E}(t)$ with a high accuracy, as is illustrated by Fig. 2(b)–(i). Meanwhile, Fig. 2(b) shows that nearly a half of $\mathcal{E}(t)$ remains unattended at $t = 25.0s$. Not later than in Fig. 2(c), the distribution of the robots becomes more uniform, with no unattended half-curve; so the body becomes surrounded from all sides. Since Fig. 2(c), the distribution is close to even, as can be seen in Fig. 2(c–j). The inter-robot distance under even distribution over the equidistant curve is set by its perimeter, which varies with time in this experiment. This is the reason for relatively large and joint oscillations of those distances in Fig. 2(j).

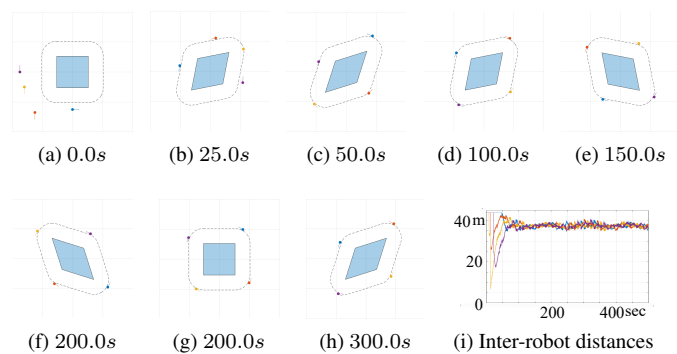


Fig. 3. A body composed of rigid moving parts.

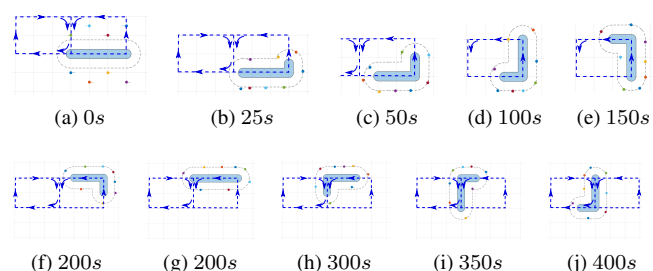


Fig. 4. Escorting a convoy.

Fig. 3 is concerned with a case where $D(t)$ is composed of rigid parts, which rotate with respect to one another. In Fig. 3, $D(t)$ is a rhombus with a fixed center and side length; the angles between adjacent sides alter with time subject to a periodic schedule. Fig. 3(a) shows the initial scene, Fig. 3(a)–(h) demonstrate snapshots taken along the subsequent maneuver. As can be seen, the control law copes with the mission and exhibits a good performance. Moreover, the final mismatch with the uniform distribution is even smaller than in Fig. 2.

Fig. 4 is inspired by the situation where several vehicles travel in a convoy one after another, and every vehicle traces the path of its predecessor at a constant distance from it. A team of escort robots should approach the convoy to a given distance and then should repeatedly encircle its entirety at this distance, not intervening between the vehicles. In Fig. 4, the convoy is modeled as a snake-like structure with a constant length. This structure traces a self-intersecting blue dashed path. As can be seen in Fig. 4, the control law copes with the mission. Meanwhile, due to frequent turns of the convoy, the distribution of the robots over the equidistant curve differs from the even one more markedly than in Fig. 2,3. Nevertheless, the convoy is eventually surrounded from all sides, as is required.

7. CONCLUSIONS

The paper presented a distributed communication-free hybrid control law that drives a group of speed- and acceleration-limited robots to a desired common distance from an unpredictably moving continuum and then ensures both tracking the respective equidistant curve in a common pre-specified direction and cluster-free distribution of the robots over this curve; this distribution is asymptotically even if the curve is steady.

REFERENCES

Ceccarelli, N., DiMarco, M., Garulli, A., and Giannitrapani, A. (2008). Collective circular motion of multi-vehicle systems.

- Automatica*, 44(12), 3025–3035.
- Deghat, M., Xia, L., Anderson, B., and Hong, Y. (2015). Multi-target localization and circumnavigation by a single agent using bearing measurements. *International Journal of Robust and Nonlinear Control*, 25(14), 2362–2374.
- Filippov, A. (1988). *Differential Equations with Discontinuous Righthand Sides*. Kluwer, Dordrecht, the Netherlands.
- Guo, J., Yan, G., and Lin, Z. (2010). Local control strategy for moving-target-enclosing under dynamically changing network topology. *Systems and Control Letters*, 59, 654–661.
- Kawakami, H. and Namerikawa, T. (2009). Cooperative target-capturing strategy for multi-vehicle systems with dynamic network topology. In *Proc. of the 2009 ACC*, 635–640. St. Louis, MO.
- Kim, T., Harab, S., and Hori, Y. (2010). Cooperative control of multi-agent dynamical systems in target-enclosing operations using cyclic pursuit strategy. *Int. J. Control*, 83(10), 2040–2052.
- Kim, T. and Sugie, T. (2007). Cooperative control for target-capturing task based on a cyclic pursuit strategy. *Automatica*, 43(8), 1426–1431.
- Kobayashi, Y. and Hosoe, S. (2011). Cooperative enclosing and grasping of an object by decentralized mobile robots using local observation. *International Journal of Social Robotics*. Available on <http://dx.doi.org/10.1007/s12369-011-0118-7>.
- Kothari, M., Sharma, R., Postlethwaite, I., Beard, R., and Pack, D. (2013). Cooperative target-capturing with incomplete target information. *International Journal of Intelligent and Robotic Systems*, 72(3–4), 373–384.
- Matveev, A. and Ovchinnikov, K. (2019). Circumnavigation of a speedy unpredictable target by a group of speed- and acceleration-limited robots. *International Journal of Robust and Nonlinear Control*, 29(4), 1063–1087.
- Matveev, A., Semakova, A., and Savkin, A. (2016). Range-only based circumnavigation of a group of moving targets by a non-holonomic mobile robot. *Automatica*, 65, 76–89.
- Matveev, A., Semakova, A., and Savkin, A. (2017). Tight circumnavigation of multiple moving targets based on a new method of tracking environmental boundaries. *Automatica*, 79, 52–60.
- Matveev, A., Wang, C., and Savkin, A. (2012). Real-time navigation of mobile robots in problems of border patrolling and avoiding collisions with moving and deforming obstacles. *Robotics and Autonomous Systems*, 60(6), 769–788.
- Ovchinnikov, K., Semakova, A., and Matveev, A. (2015). Cooperative surveillance of unknown environmental boundaries by multiple nonholonomic robots. *Robotics and Autonomous Systems*, 72, 164–180.
- Sato, K. and Maeda, N. (2010). Target-enclosing strategies for multi-agent using adaptive control strategy. In *Proc. 2010 IEEE Int. Conf. Cont. Appl.*, 1761–1766. Yokohama, Japan.
- Savkin, A., Cheng, T., Xi, Z., Javed, F., Matveev, A., and Nguyen, H. (2015). *Decentralized Coverage Control Problems for Mobile Robotic Sensor and Actuator Networks*. Wiley and IEEE Press, Hoboken, NJ.
- Spencer, J. (2004). *Continuum Mechanics*. Dover Publ., NY.
- Tsumura, K., Hara, S., Sakurai, K., and Kim, T. (2011). Performance competition in cooperative capturing by multi-agent systems. *SICE J. of Cont., Meas., Sys. Int.*, 4(3), 221–229.
- Yamaguchi, H. (2003). A distributed motion coordination strategy for multiple nonholonomic mobile robots in cooperative hunting operations. *Robotics and Aut. Systems*, 43, 257–282.